Hindawi Publishing Corporation
EURASIP Journal on Wireless Communications and Networking
Volume 2008, Article ID 348626, 9 pages
doi:10.1155/2008/348626

Research Article

Performance Evaluation of WiMAX Broadband from High Altitude Platform Cellular System and Terrestrial Coexistence Capability

Z. Yang, A. Mohammed, and T. Hult

School of Engineering, Blekinge Institute of Technology, 372 25 Ronneby, Sweden

Correspondence should be addressed to Z. Yang, zya@bth.se

Received 1 November 2007; Revised 23 April 2008; Accepted 14 August 2008

Recommended by Marina Mondin

The performance obtained from providing worldwide interoperability for microwave access (WiMAX) from high altitude platforms (HAPs) with multiple antenna payloads is investigated, and the coexistence capability with multiple-operator terrestrial WiMAX deployments is examined. A scenario composed of a single HAP and coexisting multiple terrestrial WiMAX base stations deployed inside the HAP coverage area (with radius of 30 km) to provide services to fixed users with the antenna mounted on the roof with a directive antenna to receive signals from HAPs is proposed. A HAP cellular configuration with different possible reuse patterns is established. The coexistence performance is assessed in terms of HAP downlink and uplink performance, interfered by terrestrial WiMAX deployment. Simulation results show that it is effective to deliver WiMAX via HAPs and share the spectrum with terrestrial systems.

1. INTRODUCTION

Delivering worldwide interoperability for microwave access (WiMAX) services in the 3.5 GHz band from HAPs is an effective way to provide wireless broadband communications. HAPs, recently proposed novel aerial platforms operating at an altitude of 17–22 km, have been suggested by the International Telecommunication Union (ITU) for providing communications in mm-wave broadband wireless access (BWA) and the third-generation (3G) communication frequency bands [1–3]. Investigations on HAPs have therefore been mainly concentrated in mm-wave band and code division multiple access (CDMA) schemes delivered from HAPs. HAP systems have many characteristics including high receiver elevation angle, line of sight (LOS) transmission, large coverage area, and mobile deployment. These characteristics make HAPs to be competitive to conventional terrestrial and satellite systems, and furthermore contribute to a better overall system performance, greater system capacity and cost-effective deployment.

Many countries have made significant efforts in the research of HAPs and potential applications. Some well-known projects are: (1) the HeliNet and CAPANINA projects funded by the European Union (EU) [4], (2) the SkyNet project in Japan [1], (3) a HAP project started by ETRI and KARI in Korea [5], (4) a series of research and demonstrations of HAP practical applications carried out in the U.S. by Sanswire Technologies Inc. (Fort Lauderdale, USA), and Angel Technologies [6] (St. Louis, USA). These projects mainly focus on international mobile telecommunications 2000 (IMT-2000) services, IEEE802.1x services and fixed broadband wireless access (FBWA) in different frequency bands.

WiMAX is a standard-based wireless technology for providing high-speed, last-mile BWA up to 50 km for fixed stations and 5–15 km for mobile stations in frequency bands ranging from 2 to 66 GHz [7]. In contrast, the wireless fidelity (WiFi/802.11) wireless local area network (WLAN) standards are limited in most cases to only 100–300 feet (30–100 m). WiMAX has been regarded as one of the most promising standards for delivering broadband services in the next few years and a strong competitor to the 3G system. Its standards based on IEEE 802.16a offer the potential to deliver a significantly enhanced nonline of sight (NLOS) coverage

area from HAPs in the frequency bands below 11 GHz, which leads to a more favorable propagation path due to its unique position compared with traditional base stations located on mountains or tall buildings. Providing WiMAX from HAPs is a novel approach, and some preliminary research has been done to show its effectiveness [3, 8, 9]. In this paper, we focus on the application scenario for delivering WiMAX IEEE802.16a from HAPs. In our scenarios, we assume fixed users with the directive antenna mounted on the roof to receive signals from HAPs. It is anticipated that providing WiMAX from HAPs is a competitive approach with a low deployment complexity of broadband services.

Terrestrial cellular architectures described by Lee in [10] are based on a division of the coverage area into a number of cells which are assigned to different channels with respect to adjacent cells, in order to manage cochannel interference and achieve frequency reuse. Conventionally, cells are grouped into clusters of three, four, seven, or nine cells, with all the available frequency bands allocated between them. A cluster with a larger number of cells has a greater reuse distance but fewer number of channels per cell. Previous works [8] have initially examined the fundamental performance achievable from a single-HAP and a single-terrestrial base station without considering cellular deployment for both systems. In a HAP cellular system with multiple antennas, interference is mainly caused by antennas serving cells on the same channel employing the terrestrial frequency reuse schedule [11].

This paper focuses on the system performance in different cellular reuse schemes and investigates coexistence performance with terrestrial WiMAX deployments. The paper is organized as follows. In Section 2, the description of the HAP WiMAX cellular system model, the signal path loss, and antenna models considered for HAPs and that of the terrestrial deployments is described. In Section 3, the downlink and uplink HAP WiMAX cellular system performance is evaluated in terms of criteria such as carrier to interference ratio (CIR) and carrier to interference plus noise ratio (CINR). In Section 4, a coexistence scenario is proposed to investigate the coexistence capability of HAP and terrestrial systems. In Section 5, an approach to improve HAP system performance by increasing the frequency reuse factor is shown. Conclusions are given in Section 6.

2. HAP WiMAX SYSTEM

Most of the research on HAPs considers the stratospheric platform equipped with a multiantenna payload projecting a number of spot beams within its coverage area. HAPs are employed as a group of base stations in terrestrial communication systems. A spot beam antenna architecture is able to rapidly provide a high system capacity to a number of users with a narrow beamwidth [1]. Consequently, we assume that the HAP is fitted with WiMAX base stations onboard.

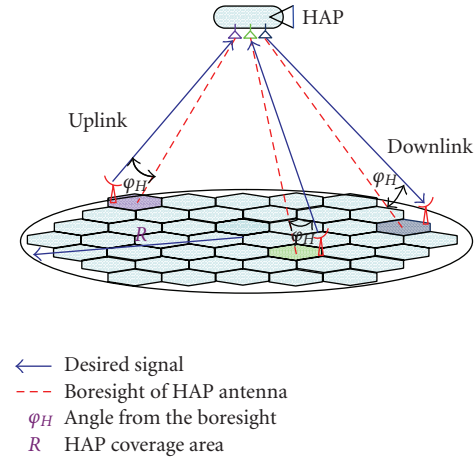

Figure 1: HAP cellular system with a multiantenna payload serving multiple cells.

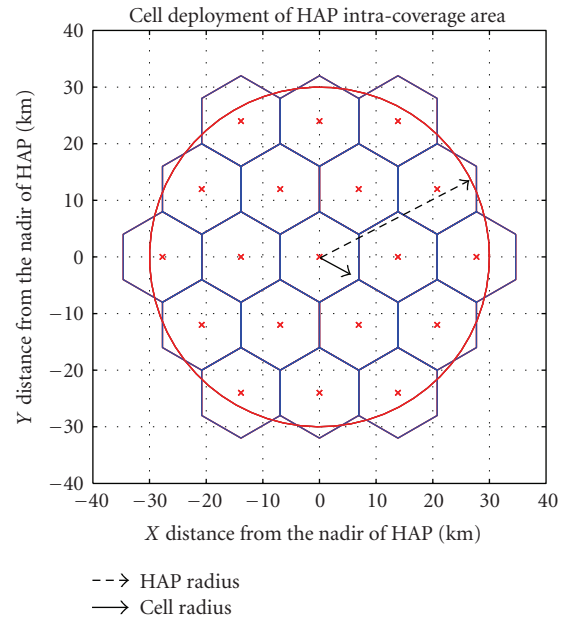

Figure 2: Plane view of cell deployment of HAP coverage area.

2.1. HAP cellular system

A scenario including a HAP cellular system is proposed in Figure 1. It consists of a single HAP with multiantenna payload at an altitude of 17 km serving multiple cells. The radius of the HAP coverage area and a HAP cell is typically 30 km and 8 km, respectively. We assume that cells are hexagonally arranged and clustered in different frequency reuse patterns to cover the HAP service area.

The receiver shown in Figure 1, which we refer to as a "user", is assumed to be located on the ground on a regular grid with one kilometer separation distance. This allows the performance of the coverage plot to be evaluated. After the performance is evaluated at one point, the user is moved

to the next point and the same simulation test is carried out again. At anytime only one user is considered to be involved in the simulation, so interference between multiple users is not taken into account. The user is located on the grid points, spaced of one kilometer in the horizontal and vertical direction. The reason of choosing the one kilometer spacing distance is that CNR or CINR does not change significantly over the distances of less than one kilometer, and also to ensure that the computation burden is not heavy especially when the coverage area is extended further.

Figure 2 shows a plane view of a HAP ground cellular deployment. Hereby, we assume a single cell radius of 8 km, which is a typical value in WiMAX system. It results in 19 cells inside the HAP coverage area. The "x" markers in Figure 2 indicate the footprints of boresight of the HAP antennas.

2.2. HAP antenna and user antenna patterns

An antenna radiation pattern is an important and critical design factor in determining the performance of radio communication systems. Ideally in cellular system, the antenna pattern would radiate uniform power across its serving cell and no power should fall outside. In practice, there is unavoidably power spilling outside the coverage area, which can cause interference to other cells.

In this paper, we employ a directive antenna pattern in [11], which can ensure more power radiated in the desired directions and decrease the power radiated towards undesired directions, on both the HAP and ground user. Antenna models are presented in (1) and (2), respectively. The gain $A_H(\varphi)$ of the HAP antennas at an angle φ with respect to its boresight, and that of the ground receiver antenna $A_U(\theta)$ at an angle θ away from its boresight are approximated by a cosine function raised to a power roll-off factor n and a notional flat sidelobe level s_f . G_H and G_U represent the boresight gain of the HAP antenna and user antenna, respectively:

$$A_H(\varphi) = G_H(\max[\cos(\varphi)^{n_H}, s_f]), \quad (1)$$

$$A_U(\theta) = G_U(\max[\cos(\theta)^{n_U}, s_f]). \quad (2)$$

The antenna peak directivity, which is usually achieved in the direction of the boresight, is assumed to be achieved at the centre of each HAP cell corresponding to its serving antenna. The boresight gain is calculated as

$$G_{\text{boresight}} = \frac{32 \ln 2}{2\theta_{3\,\text{dB}}^2}. \quad (3)$$

In this paper, the HAP antenna payload is composed of multiple antennas with the same pattern. The beamwidth $\varphi_{10\,\text{dB}}$ is initially set to be equal to the subtended angle ψ_{edge} edge at the subplatform point (SPP) with a circular beamwidth pattern as illustrated in Figure 3. This allows antenna directivities to be specified independently of the angle of the cell edge. Here, $\theta_{3\,\text{dB}}$ is the 3-dB antenna beamwidth at which the directivity curve, controlled by a roll-off factor n, is 3 dB lower than its maximum value.

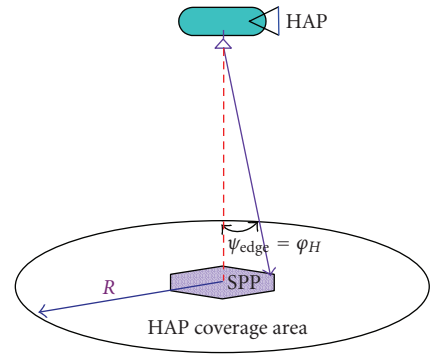

Figure 3: HAP antenna beamwidth definition.

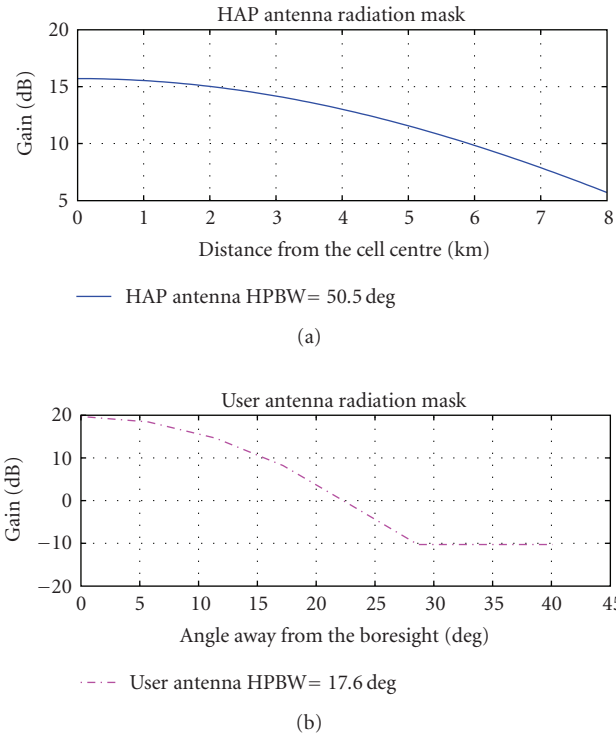

Figure 4: HAP and user antenna radiation masks.

Figure 4 shows HAP, and user antenna radiation masks defined above. Figure 5 shows the performance of the HAP antenna payload on the ground. It illustrates that the best performance is achieved at the centre, where the boresight of antenna is pointing. Since all the antennas employ the common beamwidth of the antenna serving the central cell illustrated in Figure 3, cells further away from the centre have a better performance due to a smaller subtended angle at the cell edge from its boresight.

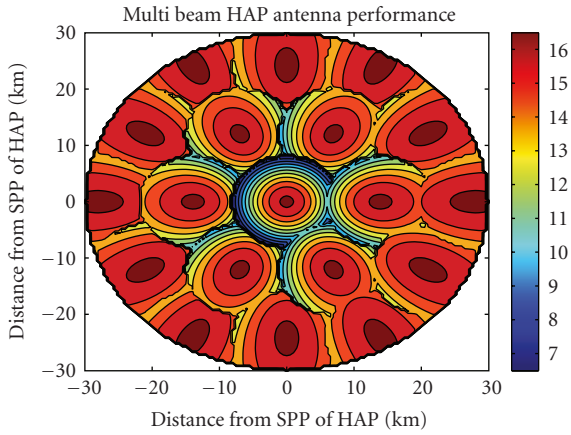

Figure 5: HAP cellular antenna payload performance.

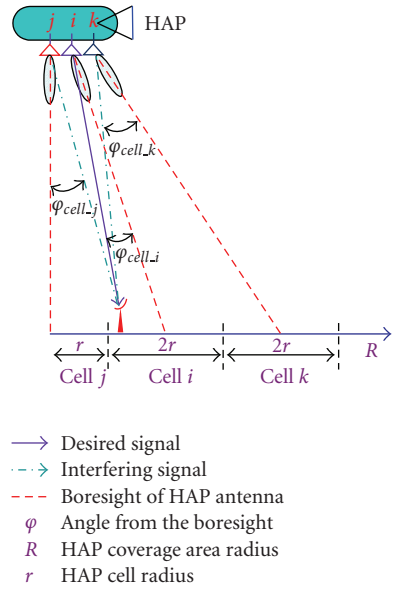

Figure 6: HAP cellular cochannel interference evaluation scenario.

2.3. HAP cellular cochannel interference evaluation

In a HAP cellular system, the interference is due to HAP antennas serving cells in the same frequency band. A cochannel interference scenario is proposed in Figure 6. The user is assumed to be located in HAP cell i. When it communicates with the HAP antenna i, the user is interfered by the HAP antenna j and k, which are assumed to operate in the same frequency band as the antenna serving the cell i. Since each HAP antenna has its boresight footprint in the centre of the corresponding cell, angles from the boresight can be calculated separately in order to access the interference.

2.4. HAP cellular reuse pattern

The WiMAX performance from a HAP cellular system is evaluated by assuming that the user inside the HAP coverage area communicates with the HAP and is interfered by the cochannel HAP antennas. In practice, a precise hexagonal pattern cannot be generated, due to topographical limitations, local signal propagation conditions, and practical limitations on sitting antennas [12].

In this paper, we use a circular shape to approximately cover the ideally proposed hexagonal pattern in HAP coverage area. The frequency reuse pattern in HAP cellular system consists of N cells assigned the same number of frequencies, which are defined as cochannel cells. N is termed as a reuse factor, which decides the number of cells in a repetitious pattern and is defined in [12]

$$N = I^2 + J^2 + (I \times J), \quad I, J = 0, 1, 2, 3, \ldots. \tag{4}$$

Hence, we test 3, 4, and 7 as possible values of N. Accordingly, the minimum distance between the cochannel cells is given as [12]

$$D = r_{\text{cell}} \cdot \sqrt{3N}. \tag{5}$$

Figure 7 shows examples of frequency reuse patterns in HAP cellular system. Cochannel cells are depicted with the same colour. Frequency reuse allows the use of same frequency already employed in other cells nearby, thus allowing frequencies to be used for multiple simultaneous communications.

2.5. Path loss calculations and simulation parameters

Currently, most HAP research papers adopt the free space path loss (FSPL) presented in (6) as the propagation model used for HAP transmission, where d is distance from the transmitter and λ is the signal wavelength. Until now, no specific propagation model has been established for HAPs at 3.5 GHz, and therefore FSPL has been widely used in current research. Propagation models have been developed for HAPs in mm-wave band at 47/48 GHz, but they are not applicable in the 3.5 GHz frequency band. It should also be noted that directional user antennas are likely to be installed at a fixed location with this scenario. High elevation angles owing to the relatively small radius of HAP coverage also mean that the LOS propagation to the HAP is a reasonable assumption. Therefore, FSPL is used in this article, and diffraction and shadowing are not explicitly considered without loss of general validity:

$$\text{PL}_H = \left(\frac{4\pi d}{\lambda}\right)^2. \tag{6}$$

The propagation pathloss model PL_T is shown in (7) for the terrestrial signal propagation model as presented in [13, 14]:

$$\text{PL}_T = \text{PL}_m + \Delta\text{PL}_f + \Delta\text{PL}_h. \tag{7}$$

PL_T is composed of a median path loss PL_m, the receiver antenna height correction term ΔPL_h and the frequency correction term ΔPL_f. The two-correction terms ΔPL_h and

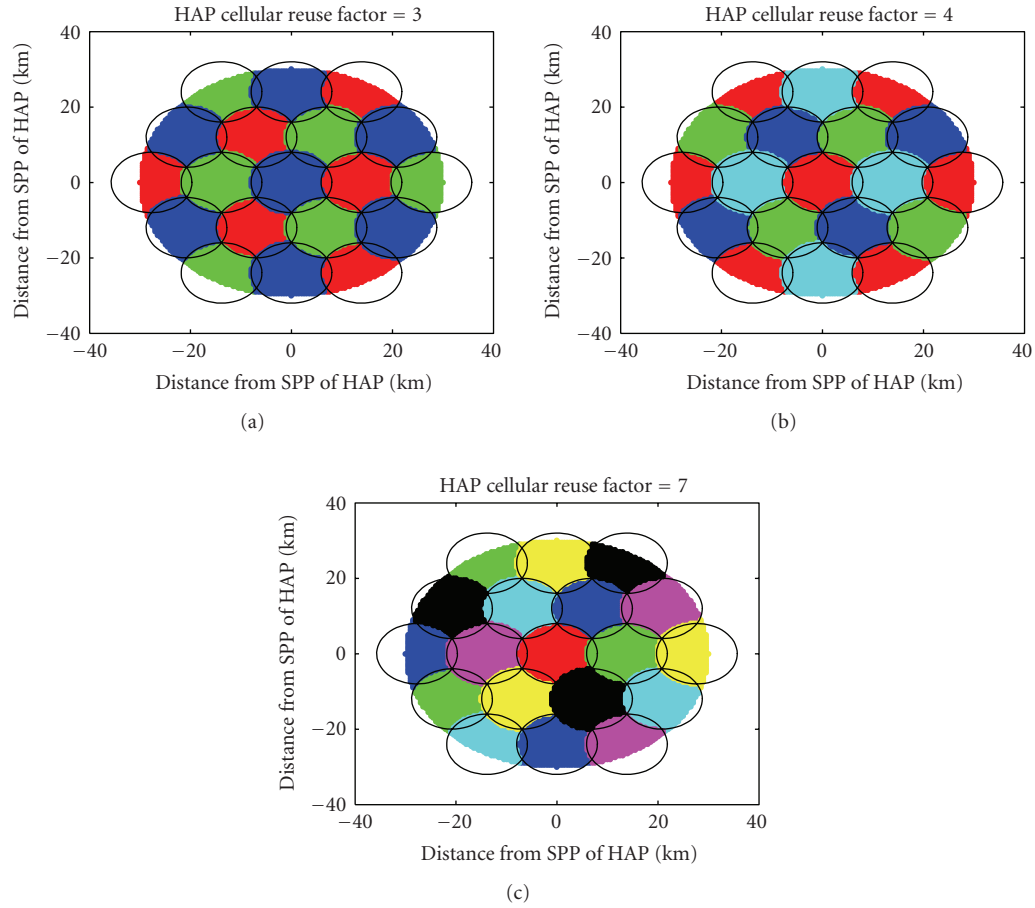

Figure 7: HAP cell layouts with the reuse factor N at 3, 4, and 7.

Table 1: Important system simulation parameters.

Parameters	HAP	Terrestrial
Coverage radius	30 km (R_H)	7 km (R_T)
Transmitter height	17 km (H_H)	30 m (H_T)
Transmitter power	40 dBm (P_H)	40 dBm (P_T)
Antenna efficiency	80%	
User roll-off rate	58 (n_U)	
User boresight gain	18 dB (G_U)	
Sidelobe level	−30 dB (s_f)	
Bandwidth	7 MHz/1.75 MHz (DL/UL)	
Frequency	3.5 GHz	

ΔPL_f [15] are added in order to make PL_T more accurate by accounting for the antenna heights and frequencies. In this paper, parameters in suburban environment (category C [13]) are used for simulations of a terrestrial deployment environment. We assume that the HAP carries the multi-antenna payload with a radiation pattern described in (1) and the terrestrial base stations use omnidirectional antennas. Table 1 shows the most important system parameters for downlink (DL) and uplink (UL) simulations.

3. HAP CELLULAR SYSTEM PERFORMANCE

3.1. HAP downlink system performance evaluation

A user in a location (x, y) is considered to be communicating with its serving HAP antenna and to be receiving interference signals from other antennas operating in the same frequency band. Performance can be evaluated as a function of CIR and CINR in (8) and (9), respectively:

$$\mathrm{CIR}_H(x,y) = \frac{P_H A_H A_U \mathrm{PL}_{HU}}{\sum_{i=1}^{N_H} P_{H_i} A_{H_i} A_{U_i} \mathrm{PL}_{H_i U}}, \tag{8}$$

$$\mathrm{CINR}_H(x,y) = \frac{P_H A_H A_U \mathrm{PL}_{HU}}{N_F + \sum_{i=1}^{N_H} P_{H_i} A_{H_i} A_{U_i} \mathrm{PL}_{H_i U}}, \tag{9}$$

where

(i) P_H is the transmission power of the HAP transmitter;

(ii) P_{Hi} is the transmission power of the interfering HAP antennas;

(iii) A_H and A_U are the antenna gains of the HAP and the user, and they depend on the angular deviation from the boresight;

(iv) PL_{HU} is the propagation pathloss from HAP to user;

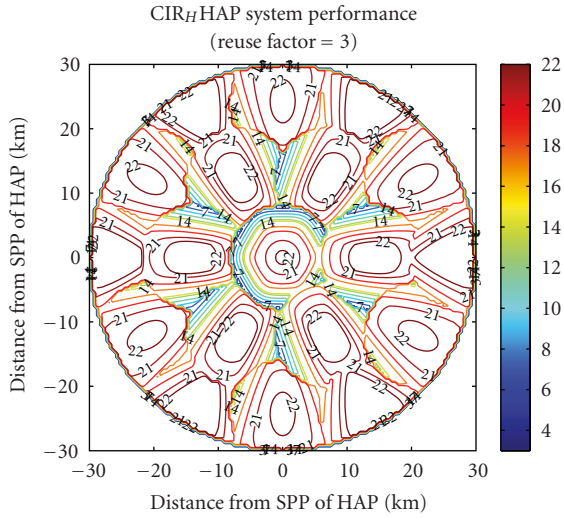

Figure 8: CIR performance of a HAP WiMAX system with reuse factor = 3.

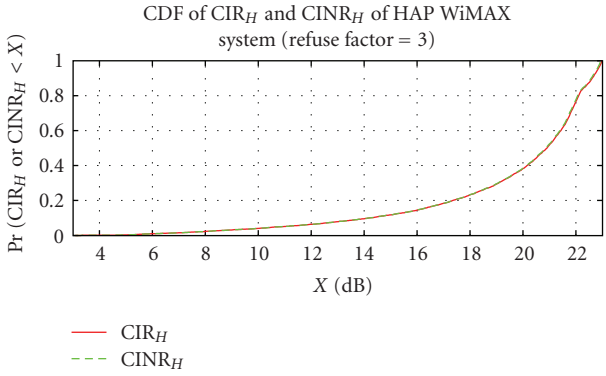

Figure 9: CDF of CIR and CINR performance of a HAP WiMAX system with reuse factor = 3.

(v) N_H is the total number of cochannel cells in the HAP system;

(vi) N_F is the noise power (-100.5 dBm).

Figure 8 illustrates the CIR performance in the HAP coverage area when considering the cochannel interference. Contours inside each cell have approximately the same shape as that in Figure 5, which demonstrates that cellular performance is not susceptible to cochannel interference.

Figure 9 shows the cumulative distribution function (CDF) of CIR$_H$ and CINR$_H$ of a HAP WiMAX system. It can be seen that WiMAX services can be provided on average 21 dB in both scenarios with values of CIR or CINR larger or equal to 21 dB. Interference from cochannel is dominant compared to noise in the system since the curves in Figure 9 are overlapping. Hence, strategies for system performance improvement should mainly focus on reducing excess power from cochannel interference.

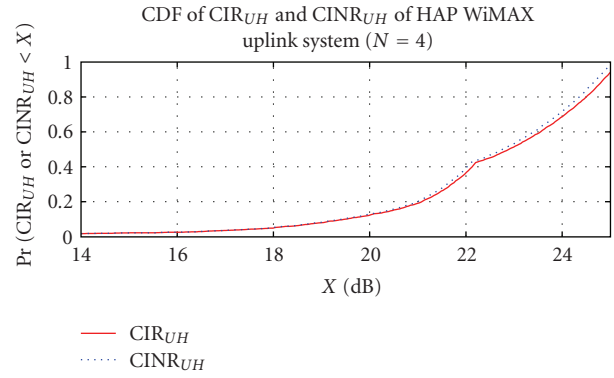

Figure 10: CDF of uplink CIR and CINR performance in a HAP uplink system with reuse factor = 4.

3.2. HAP uplink system performance evaluation

Uplink performance of a HAP WiMAX system can be evaluated by considering a user in a location (x, y) communicating with its serving HAP antenna and other antennas serving other cells in the same frequency band. CIR and CINR can be expressed as

$$\mathrm{CIR}_{UH}(x,y) = \frac{P_U A_U A_H \mathrm{PL}_{UH}}{\sum_{i=1}^{N_H} P_U A_{U_i} A_{H_i} \mathrm{PL}_{UH_i}},$$
$$\mathrm{CINR}_{UH}(x,y) = \frac{P_U A_U A_H \mathrm{PL}_{UH}}{N_F + \sum_{i=1}^{N_H} P_U A_{U_i} A_{H_i} \mathrm{PL}_{UH_i}}, \quad (10)$$

where

(i) P_U is the transmission power of user in the target cell (30 dBm);

(ii) PL_{UH} is the propagation pathloss from user to HAP;

(iii) N_F is the noise power (-106.5 dBm).

Figure 10 shows the CDF of uplink CIR and CINR of HAP WiMAX system. It can be seen that WiMAX uplink services can be provided averagely around 22 dB in both cases. Cochannel interference is also dominant compared to noise.

4. PERFORMANCE OF A HAP COEXISTENCE SCENARIO

Providing WiMAX from HAPs is a novel means to deliver broadband services. Thus, it is vital to consider its coexistence capability with current terrestrial WiMAX system in order to get an assessment of the performance. In this paper, we mainly focus on evaluating interference from terrestrial WiMAX to the HAP system.

4.1. HAP coexistence scenario

The considered coexistence model is depicted in Figure 11. We assume that the terrestrial WiMAX system employs the same cellular configuration as the HAP system. There

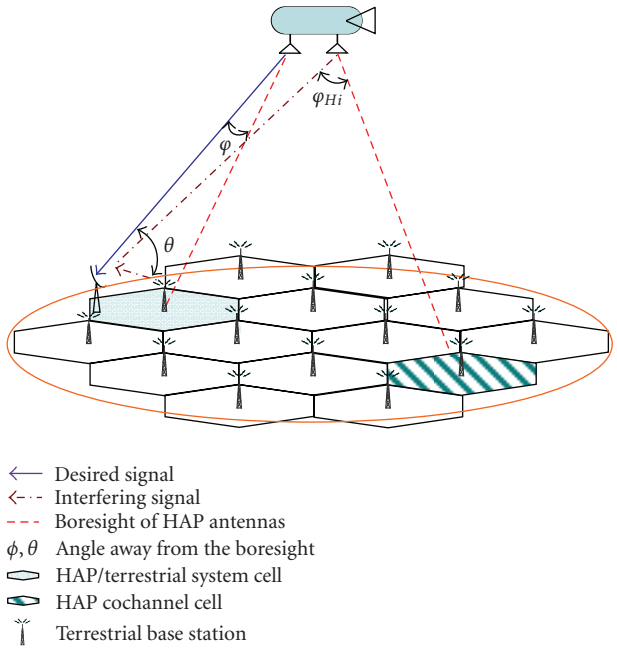

Figure 11: Coexistence model of HAP and terrestrial WiMAX system.

are therefore 19 terrestrial base stations considered in the scenario, and all the base stations are located in the centre of HAP cells. A user communicating with the HAP in an arbitrary HAP cell is interfered by the HAP cochannel antennas and the terrestrial base station located in the centre of the same cell. This scenario, in which a user always receives interference from its nearest terrestrial base station, can be regarded as the worst case, since interfering terrestrial base station is further away from the user if any different reuse pattern was adopted.

4.2. HAP downlink coexistence scenario

Downlink coexistence performance of HAP and terrestrial systems can be assessed by evaluating the CIR as

$$\mathrm{CIR}_{HT}(x,y) = \frac{P_H A_H A_U \mathrm{PL}_{HU}}{\sum_{i=1}^{N_H} P_{H_i} A_{H_i} A_{U_i} \mathrm{PL}_{H_i U} + P_T A_T A_{UT} \mathrm{PL}_{TU}}, \tag{11}$$

where

(i) P_T is the transmission power of the interfering terrestrial base station;

(ii) PL_{TU} is the pathloss from the terrestrial base station to user;

(iii) A_{UT} is the user antenna gain at an angle away from its boresight.

In Figure 12, the uplink contour plot clearly shows that in most of the cell areas HAP system can provide stable services to the users, regardless of interference from the terrestrial system.

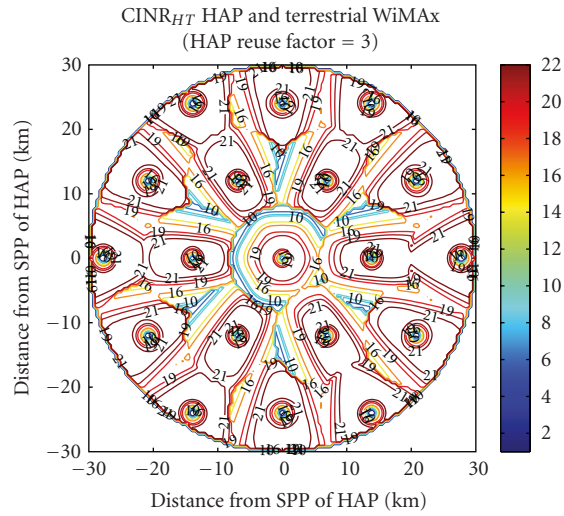

Figure 12: DL HAP system performance of user interfered by terrestrial deployments.

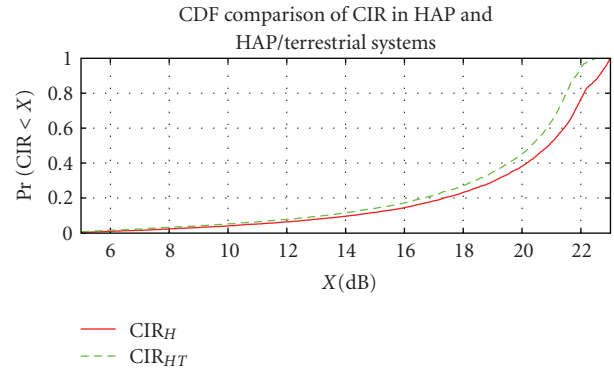

Figure 13: Comparison of the DL CIR values in HAP (CIR_H) and HAP/terrestrial (CIR_{HT}) WiMAX coexistence scenarios.

Figure 13 shows the CDF of the CIR value in the HAP and the coexistence scenario, respectively. On average, the HAP system can be operated with a CIR larger or equal to 21 dB, but a slight decrease in performance in the coexistence scenario can be observed because of the interference from the terrestrial system.

4.3. HAP uplink coexistence evaluation

Uplink coexistence performance of HAP and terrestrial systems can be assessed by evaluating the CIR as

$$\mathrm{CIR}_{HT}(x,y) = \frac{P_U A_U A_H \mathrm{PL}_{UH}}{\sum_{i=1}^{N_H} P_U A_{U_i} A_{H_i} \mathrm{PL}_{UH_i} + P_U A_U A_T \mathrm{PL}_{UT}}, \tag{12}$$

where

(i) PL_{UT} is the propagation path loss from the user to the terrestrial base station.

Figure 14 shows the contour plot of the uplink coexistence scenario of the HAP system. In most of cell areas, the

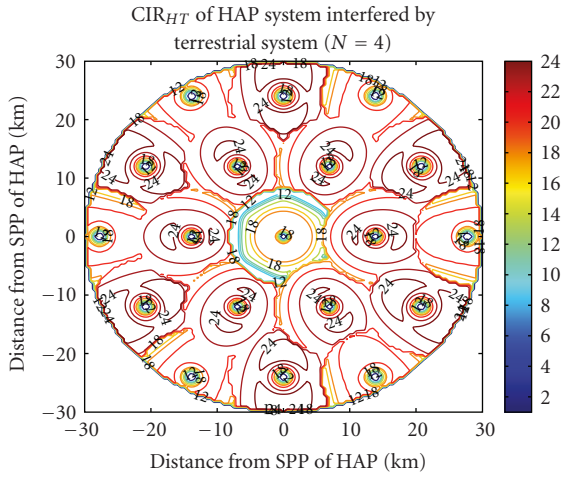

FIGURE 14: UL CIR value of HAP system (CIR$_{HT}$) interfered by the terrestrial system.

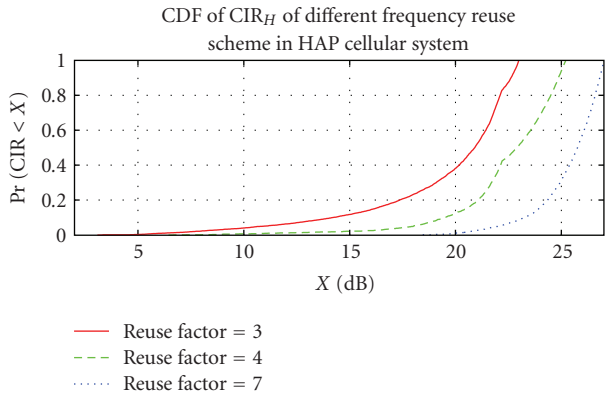

FIGURE 15: DL CIR$_H$ performance of HAP system with different values of the reuse factor N (3, 4, and 7).

HAP can provide stable uplink services to users, which are not susceptible to interference from the terrestrial system.

5. HAP WiMAX SYSTEM IMPROVEMENT

A number of approaches have been used to improve the cellular system performance, for example, adding new channels, cell splitting, cell sectoring. Increasing D, the minimum distance between cochannel cells, is an effective approach, since it can keep the cochannel cells further away from each other and therefore decrease the interference without requiring more spectrum.

Figure 15 shows the downlink CIR$_H$ performance of the HAP system for different values of D, obtained by increasing the reuse factor N. It shows that a CIR increase of approximately 2 dB can be achieved with each increment of N in the figure (from 3 to 4, or from 4 to 7). Usually the total number of frequencies allotted to the system is constant, so increasing D, on the other hand, decreases available channel resources in each cell of the system.

6. CONCLUSIONS

In this paper, we have shown the performance of both downlink and uplink WiMAX broadband standard transmitted from a HAP cellular system in the 3.5 GHz band across a coverage area of 30 km radius, while operating in the same frequency band with terrestrial WiMAX deployments based on a proposed coexistence scenario. A cellular configuration has been proposed for the HAP WiMAX system based on the typical WiMAX terrestrial system. The HAP coverage area was divided into 19 individual cells served by multiantenna payload. WiMAX broadband system performance of individual HAP system was evaluated both separately and when taking into account the cochannel interference from the antennas operating in the same frequency band. Coexistence capability was investigated based on a proposed coexistence scenario and examined by considering interference from the nearest terrestrial base station to HAP system. Simulation results clearly demonstrate that the internal cochannel interference was dominant when delivering WiMAX via HAPs, and HAP system can effectively share the spectrum with terrestrial WiMAX systems.

REFERENCES

[1] J.-J. Huang, W.-T. Wang, and H.-W. Ferng, "Uplink capacity enhancement for an integrated HAPS-terrestrial CDMA system," *IEEE Communications Letters*, vol. 11, no. 1, pp. 10–12, 2007.

[2] Z. E. O. Elshaikh, R. Islam, A. P. Ismail, and O. O. Khalifa, "High altitude platform for wireless communications and other services," in *Proceedings of the 4th International Conference on Electrical and Computer Engineering (ICECE '06)*, pp. 432–438, Dhaka, Bangladesh, December 2006.

[3] B. T. Ahmed, "WiMAX in high altitude platforms (HAPs) communications," in *Proceedings of the 9th European Conference on Wireless Technology (ECWT '06)*, pp. 245–248, Manchester, UK, September 2006.

[4] D. Grace, M. Mohorcic, M. Oodo, M. H. Capstick, M. B. Pallavicini, and M. Lalovic, "CAPANINA—communications from aerial platform networks delivering broadband information for all," in *Proceedings of the 14th IST Mobile and Wireless and Communications Summit*, Dresden, Germany, June 2005.

[5] J.-M. Park, B.-J. Ku, Y.-S. Kim, and D.-S. Ahn, "Technology development for wireless communications system using stratospheric platform in Korea," in *Proceedings of the 13th IEEE International Symposium on Personal, Indoor and Mobile Radio Communications (PIMRC '02)*, vol. 4, pp. 1577–1581, Lisbon, Portugal, September 2002.

[6] T. C. Hong, B. J. Ku, J. M. Park, D.-S. Ahn, and Y.-S. Jang, "Capacity of the WCDMA system using high altitude platform stations," *International Journal of Wireless Information Networks*, vol. 13, no. 1, pp. 5–17, 2006.

[7] IEEE802.16 Broadband Wireless Access Working Group, "IEEE802.16-2004 part 16: air interface for fixed broadband wireless access system," October 2004.

[8] P. Likitthanasate, D. Grace, and P. D. Mitchell, "Coexistence performance of high altitude platform and terrestrial systems sharing a common downlink WiMAX frequency band," *Electronics Letters*, vol. 41, no. 15, pp. 858–860, 2005.

[9] Z. Yang, A. Mohammed, T. Hult, and D. Grace, "Optimizing downlink coexistence performance of WiMAX services in

HAP and terrestrial deployments in shared frequency bands," in *Proceedings of the 3rd International Waveform Diversity and Design Conference (WDD '07)*, pp. 79–82, Pisa, Italy, June 2007.

[10] W. C. Y. Lee, "Spectrum efficiency in cellular," *IEEE Transactions on Vehicular Technology*, vol. 38, no. 2, pp. 69–75, 1989.

[11] J. Thornton, D. Grace, M. H. Capstick, and T. C. Tozer, "Optimizing an array of antennas for cellular coverage from a high altitude platform," *IEEE Transactions on Wireless Communications*, vol. 2, no. 3, pp. 484–492, 2003.

[12] W. Stallings, *Wireless Communications and Networking*, Prentice-Hall, Upper Saddle River, NJ, USA, 2002.

[13] IEEE Standard 802.16a-2003, "Modifications and additional physical layer specifications for 2-11 GHz," 2003.

[14] V. Erceg, L. J. Greenstein, S. Y. Tjandra, et al., "An empirically based path loss model for wireless channels in suburban environments," *IEEE Journal on Selected Areas in Communications*, vol. 17, no. 7, pp. 1205–1211, 1999.

[15] IEEE802.16 Broadband Wireless Access Working Group, "Channel models for fixed wireless applications," June 2003.